THE JOURNAL OF BIOLOGICAL CHEMISTRY VOL. 287, NO. 27, pp. 22827–22837, June 29, 2012

Polymorphism of β_2-Microglobulin Amyloid Fibrils Manifested by Ultrasonication-enhanced Fibril Formation in Trifluoroethanol*[S]

Received for publication, December 12, 2011, and in revised form, April 16, 2012 Published, JBC Papers in Press, May 7, 2012, DOI 10.1074/jbc.M111.333310

Eri Chatani[‡§1], **Hisashi Yagi**[§], **Hironobu Naiki**[¶], **and Yuji Goto**[§]

From the [‡]*Department of Chemistry, Graduate School of Science, Kobe University, Hyogo 657-8501, Japan, the* [§]*Institute for Protein Research, Osaka University, Osaka 565-0871, Japan, and the* [¶]*Division of Molecular Pathology, Department of Pathological Sciences, Faculty of Medical Sciences, University of Fukui, Fukui 910-1193, Japan*

Background: Polymorphism of amyloid fibrils underlies the manifestation of different phenotypes of amyloidoses.
Results: Various types of β_2-microglobulin fibrils were formed in 2,2,2-trifluoroethanol in a concentration-dependent manner.
Conclusion: The relationship between fibril properties and TFE concentration suggests a critical role of hydrophobic interactions for polymorphism.
Significance: The modulation of hydrophobic interactions will become a novel strategy for regulating amyloid diseases at a molecular level.

The polymorphic property of amyloid structures has been focused on as a molecular basis of the presence and propagation of different phenotypes of amyloid diseases, although little is known about the molecular mechanism for expressing diverse structures from only one protein sequence. Here, we have found that, in combination with an enhancing effect of ultrasonication on nucleation, β_2-microglobulin, a protein responsible for dialysis-related amyloidosis, generates distinct fibril conformations in a concentration-dependent manner in the presence of 2,2,2-trifluoroethanol (TFE). Although the newly formed fibrils all exhibited a similar needle-like morphology with an extensive cross-β core, as suggested by Fourier transform infrared absorption spectra, they differed in thioflavin T intensity, extension kinetics, and tryptophan fluorescence spectra even in the same solvents, representing polymorphic structures. The hydrophobic residues seemed to be more exposed in the fibrils originating at higher concentrations of TFE, as indicated by the increased binding of 1-anilinonaphthalene-8-sulfonic acid, suggesting that the modulation of hydrophobic interactions is critical to the production of polymorphic amyloid structures. Interestingly, the fibrils formed at higher TFE concentrations showed significantly higher stability against guanidium hydrochloride, the perturbation of ionic strength, and, furthermore, pressurization. The cross-β structure inside the fibrils seems to have been more idealized, resulting in increased stability when nucleation occurred in the presence of the alcohol, indicating that a weaker contribution of hydrophobic interactions is intrinsically more amenable to the formation of a non-defective amyloid structure.

Amyloid fibrils are supramolecular assemblies of proteins often associated with serious disorders such as Alzheimer's disease, prion disease, Parkinson's disease, and dialysis-related amyloidosis (1–4). The most characteristic feature of amyloid fibrils independent of protein sequences is a cross-β structure where β-strands align perpendicularly to the fibril axis. However, recent experimental studies have revealed that, despite this apparent similarity in morphology, a variety of fibril conformations are formed even from one protein sequence, which leads to differences in pathology and transmission. For yeast prion Sup35, amyloid fibrils formed *in vitro* with conformational variations induced distinct prion strains that further propagated to the subsequent generations (5). For β-amyloid fibrils responsible for Alzheimer's disease (6) and huntingtin exon1-possessing expanded polyglutamines responsible for Huntington disease (7), amyloid fibrils with distinct conformations showed different neurotoxic effects on living cells. Given these findings, understanding the polymorphic nature of amyloid fibrils is essential to elucidating the pathogenesis and transmission of amyloidoses at a molecular level (8).

In many cases, the structural diversity of amyloid fibrils is manifested as morphological diversity with respect to flexibility in shape, repeat distance of twists, and fibril length and width. Although some of this morphological diversity may emerge simply from differences in the hierarchical assembly of a single type of protofilament (9), recent research has revealed microscopic structural diversity underlying each protofilament, such as the amount of cross-β core, parallel/antiparallel alignment of β-strands, protofilament core topology, and, additionally, more minute structural variety observed at an amino acid level, as detected by using hydrogen/deuterium exchange NMR spectroscopy (10, 11), solid-state NMR spectroscopy (12–15), cryo-EM (16), x-ray crystallography with microcrystals (17, 18), and Fourier transform infrared spectroscopy (19, 20). For a comprehensive understanding and for regulation of the structure and function of each type of amyloid fibril, elucidation of the interactions inside the polypeptide chains constituting the

* This work was supported in part by Japanese Ministry of Education, Culture, Sports, Science, and Technology Scientific Research Grant-in-Aid 21370044 and Young Scientists Grant-in-Aid 23770188 and by Japan Society for the Promotion of Science Research Activity Start-up Grant-in-Aid 22810014.

[S] This article contains supplemental Figs. S1–S5 and Experimental Procedures.

[1] To whom correspondence should be addressed: Department of Chemistry, Graduate School of Science, Kobe University, 1-1 Rokkodai, Kobe, Hyogo 657-8501, Japan. Tel.: 81-78-803-5673; Fax: 81-78-803-5673; E-mail: chatani@crystal.kobe-u.ac.jp.

fibrils is essential. However, unlike the amount of information available regarding the native globular structure, much remains to be elucidated, in particular the key interactions determining the physicochemical properties of amyloid fibrils. The mechanism that accounts for multiple conformations from one unique amino acid sequence needs to be clarified.

Here, we address our new finding that multiple forms of amyloid fibrils of β_2-microglobulin (β2-m)[2] are produced on the addition of 2,2,2-trifluoroethanol (TFE) in a concentration-dependent manner. β2-m, a light chain of the type I major histocompatibility antigen (MHC-1) with 99 amino acid residues, is the main component of the amyloid fibrils deposited in patients with dialysis-related amyloidosis (21, 22). We have previously clarified that alcohols, in particular TFE and hexafluoroisopropanol, markedly accelerated the formation of fibrils by a 22-residue fragment of β2-m (K3 peptide) and human islet amyloid polypeptide (23, 24). This acceleration was eminent, especially at concentrations slightly below the alcohol clustering concentration, exhibiting a bell-shaped dependence on the concentration of alcohol as a result of a balancing of hydrophobic and electrostatic interactions. At higher concentration of alcohol, the weak polarity of the solvent is resistant to fibril formation, alternatively stabilizing α-helical structures with extended intramolecular hydrogen networks in many cases. Curiously, we have found that β2-m amyloid fibrils can be formed even at TFE concentrations above the alcohol clustering concentration if combined with ultrasonication.

Ultrasonication is an effective agitating system with intensive effects on the spontaneous formation of amyloid fibrils with a short lag time of only several hours by reducing the free-energy barrier of nucleating processes (25–27). Although few β2-m fibrils form under quiescent conditions because of the high energetic barrier, we have clarified that ultrasonication strongly generates β2-m amyloid fibrils without any seeds (25–27). With the assistance of this effect, we obtained a series of polymorphic fibrils at various concentrations of TFE. Interestingly, the fibrils generated at higher concentration of TFE were more stable. On the basis of the physicochemical properties of the amyloid fibrils obtained, the molecular mechanism underlying the manifestation of this polymorphism will be discussed.

EXPERIMENTAL PROCEDURES

Expression and Purification of β2-m—Recombinant human β2-m was produced with an *Escherichia coli* expression system as described previously (28). The purified β2-m was desalted by dialysis against deionized water and stocked as a lyophilized form for experiments. Concentrations of monomeric β2-m were determined using an absorption coefficient of 19,300 $cm^{-1}{}_M{}^{-1}$ at 280 nm (28).

Ultrasonication-induced Fibril Formation—To induce the spontaneous formation of β2-m amyloid fibrils without seeds, the ultrasonication system established in our previous study was used (25–27). Samples of 0.3 mg/ml of β2-m dissolved in 10 mM HCl containing 100 mM NaCl and various concentrations of TFE (0–50%) were placed on a water bath-type ultrasonic transmitter with a temperature controller (ELESTEIN SP070-PG-M, Elekon, Tokyo). The concentration of TFE was represented by v/v. The pH of the solutions with 10 mM HCl in the absence of TFE was 2.0. Although TFE increases the pH because of its hydrophobic effects, we did not try to keep the pH constant because increasing the HCl concentration complicates the experimental conditions. The temperature of the samples was maintained at 37 °C, ultrasonication was applied for 1 min, and then the samples were incubated for 9 min without sonication, a process that was repeated. The samples were ultrasonicated from three directions, *i.e.* the bottom and two walls of the incubating bath, the ultrasonication pulses from which cross one another at the sample position (25–27). The frequency and the power of output of the sonication were 17–20 kHz and 350 watts, respectively. At different points of time, a 5-μl aliquot of sample was mixed with 1 ml of 5 μM ThT in 50 mM glycine-NaOH buffer (pH 8.5) at 25 °C, and the fluorescence intensity at 485 nm of this solution was measured with an excitation wavelength of 445 nm to monitor the formation of amyloid fibrils (29).

Seed-dependent Fibril Extension—The seed-dependent extension reaction was examined according to the method of Naiki *et al.* (29) with a slight modification of the solutions. β2-m was dissolved at a concentration of 0.3 mg/ml in a 10 mM HCl solution containing 100 mM NaCl and various concentrations of TFE (0–50%) in the presence of 30 μg/ml of ultrasonicated fibrils as seeds. For the preparation of seeds, fibrils were ultrasonicated using a Microson sonicator (Misonix, Farmingdale, NY) at intensity level 2 and 20 1-s pulses. The extension reaction was carried out at 37 °C without agitation and monitored at different points in time by measuring ThT fluorescence. In the repeated self-seeding experiments, β2-m fibrils produced by ultrasonication (F0) were used as the first seeds (S0) to make F1 fibrils. By repeating the protocol, F2, F3, F4, and F5 fibrils were obtained from the seed-dependent formation of fibrils with S1, S2, S3, and S4 seeds, respectively, as described previously (30). For S0 seeds, no ultrasonication was applied for fragmentation. The extension reaction in the same solvent was also carried out with fundamentally the same method as that described above, where the TFE concentration was uniformly set to 5%.

Transmission Electron Microscopy—Amyloid fibrils (0.3 mg/ml) were diluted 20-fold with water and immediately placed on carbon-coated copper grids (400 mesh). The excess solution was removed with filter paper after the sample had stood for 1 min, and the fibrils adsorbed on the grid were negatively stained with a 2% (w/v) uranyl acetate solution. Electron micrographs were acquired using a transmission electron microscope (100CX, JEOL, Tokyo, Japan) at 80 kV with a magnification of ×29,000.

Measurement of Circular Dichroism—Far-UV circular dichroism (CD) spectra were measured with a J-600 model spectropolarimeter (Jasco, Japan). Samples (0.15 mg/ml) of the monomer or amyloid fibrils of β2-m in 10 mM HCl containing 0.1 M NaCl and various concentrations of TFE were analyzed. For the analysis of amyloid fibrils, samples dissolved in 10 mM HCl containing 5% TFE and 0.1 M NaCl were also prepared and measured. Measurements were performed at 25 °C with a path

[2] The abbreviations used are: β2-m, β_2-microglobulin; TFE, 2,2,2-trifluoroethanol; ThT, thioflavin T; ANS, 1-anilinonaphthalene-8-sulfonic acid; Gdn-HCl, guanidine hydrochloride; FTIR, Fourier transform infrared.

length of 0.1 cm, and the results were expressed as mean residue ellipticity [θ].

FTIR Absorption Measurement—Attenuated total reference FTIR spectra were measured with a J-6100 model spectrometer (Jasco, Japan) with an attenuated total reference option. Fibrils formed by seed-dependent extension reaction were precipitated by centrifugation and resuspended by a small amount of the same solvents to concentrate the fibrils to ~2 mg/ml, and then 2 μl of them were loaded and dried on the attenuated total reference prism for the measurement. FTIR spectra were then monitored at room temperature with a resolution of 4 cm^{-1}. The spectra were normalized so that the integrated intensity of the amide I band ranging from 1580 to 1750 cm^{-1} was set to be equal.

Spectral Analysis of Tryptophan Fluorescence—Tryptophan fluorescence spectra of the fibrillar forms of β2-m were measured using a Hitachi F-4500 fluorescence spectrophotometer. Fibrils at 0.05 mg/ml were incubated at 25 °C for 5 min in the thermostated cuvette holder of the spectrophotometer, and fluorescence spectra from 310 to 440 nm were collected with an excitation wavelength of 295 nm.

Binding of 1-Anilinonaphthalene-8-sulfonic Acid—Fibrils at a concentration of 0.05 mg/ml were reacted with 25 μM 1-anilinonaphthalene-8-sulfonic Acid (ANS) in 10 mM HCl containing 0.1 M NaCl and 5% TFE at 25 °C for 1 h. After the reaction, the fluorescence spectra of ANS within the samples were measured from 400 to 600 nm with an excitation at 350 nm.

Stability of β2-m Amyloid Fibrils against Guanidine Hydrochloride, at Neutral pH, and at Low Ionic Strength—The stability of β2-m amyloid fibrils in the presence of guanidine hydrochloride (Gdn-HCl) was examined by monitoring the equilibrium depolymerization of β2-m amyloid fibrils on the basis of the change in intrinsic tryptophan fluorescence. The fibrils were suspended at a concentration of 0.05 mg/ml in 10 mM HCl containing 0.1 M NaCl, 5% TFE, and various concentrations of Gdn-HCl, which were incubated at 25 °C for 1 day before the measurements. Each spectrum was quantified using the center of spectral mass, $<\nu>$, the average energy of fluorescence spectra calculated from the following equation,

$$<\nu> = \Sigma \nu_i \times F_i / \Sigma F_i \qquad \text{(Eq. 1)}$$

where ν_i and F_i are the wavenumber and fluorescence intensity at ν_i (31).

The stability of β2-m amyloid fibrils at neutral pH or low ionic strength was examined by monitoring the time course of depolymerization reactions. Amyloid fibrils of β2-m were first prepared by incubating 1.2 mg/ml of monomeric β2-m in 10 mM HCl containing 0.1 M NaCl, 5% TFE, and 30 μg/ml of seeds at 37 °C. The fibrils were then diluted 6-fold with a 50 mM sodium phosphate buffer containing 0.1 M NaCl to raise the pH to 7.0 or 24-fold with a 10 mM HCl solution to decrease the NaCl concentration to 4.2 mM. The reactions were monitored by measuring ThT fluorescence at different points of time.

RESULTS

Formation of β2-m Amyloid Fibrils in the Presence of TFE—First we examined the effects of TFE on the formation of β2-m amyloid fibrils by monitoring the reaction at concentrations of TFE from 0 to 50%. β2-m forms amyloid fibrils from an acid-unfolded state at low pH *in vitro*, which we adopted as standard conditions. In a 10 mM HCl solution containing 0.1 M NaCl, standard conditions in this study, monomeric β2-m was acid-unfolded, showing a far-UV CD spectrum with a minimum at 205 nm (Fig. 1*A*, *inset*). The addition of TFE induced the formation of an α-helical structure with a minimum at 208 nm and a shoulder at 222 nm and the structural transition saturated at 30% TFE and above in a similar fashion to that observed in 20 mM HCl (32) (Fig. 1*A*, *inset*). These β2-m monomers were then placed in a thermoregulated water bath at 37 °C and ultrasonicated repeatedly for 1 min every 10 min to enhance fibrillation. Under the standard conditions without TFE, a rapid increase in ThT fluorescence was observed after a lag time of about 4 h, as observed previously (Fig. 1*A*) (25–27). An unambiguous increase in ThT fluorescence was also observed under all of the conditions in the presence of 10–50% TFE, suggesting that the formation of amyloid fibrils occurs even in the presence of relatively high concentrations of TFE, although more time is required (Fig. 1*A*). The ultrasonication-induced fibrillation reactions showed fairly good reproducibility in terms of the overall shape of the kinetics and the final ThT intensity under all conditions at different concentrations of TFE, although some fluctuations were observed in the presence of 20% TFE. The final value for fluorescence intensity was generally smaller in the presence of TFE than in its absence. The length of the lag phase increased significantly as the concentration of TFE increased, and growth after the lag phase also seemed to decelerate significantly in the presence of TFE, especially at 40 and 50% TFE. The control reaction without applying ultrasonication pulses did not exhibit any increase in ThT fluorescence for all samples within the experimental period (see supplemental Fig. S1).

To verify the formation of amyloid fibrils at different concentrations of TFE, we analyzed the ability to self-propagate, a characteristic feature of amyloid fibrils, by monitoring seed-dependent extension reactions with the sonication-generated fibrils as seeds. It should be noted that the seed-dependent extension reactions hereafter were carried out without ultrasonication. When sonication-generated amyloid fibrils were added to a newly prepared monomeric β2-m solution containing the same TFE concentration as that present during the nucleation, ThT fluorescence increased dramatically in an exponential manner without a lag phase for all fibrils (Fig. 1*B*), from which we concluded that amyloid fibrils were formed at all concentrations of TFE. Repeated cycles of self-seeding produced second, third, and fourth (which was analyzed only at 10%) generations of fibrils, with some acceleration of the extension reaction observed in the second cycle at 30 and 40% but no change observed at 0%, 10%, 20%, or 50% (Fig. 1*B*). Considering that the final ThT fluorescence at 30 and 40% was dramatically increased after the seed-dependent extension reactions (Fig. 1, *A* and *B*), it is plausible that the first generation of fibrils at 30 and 40% contained a fraction of amorphous aggregates or fibrils with very low ThT fluorescence and weak seeding ability. Finally, the amyloid fibrils obtained by the nucleation and subsequent repeated self-seeding at 0, 10, 20, 30, 40, and 50% TFE

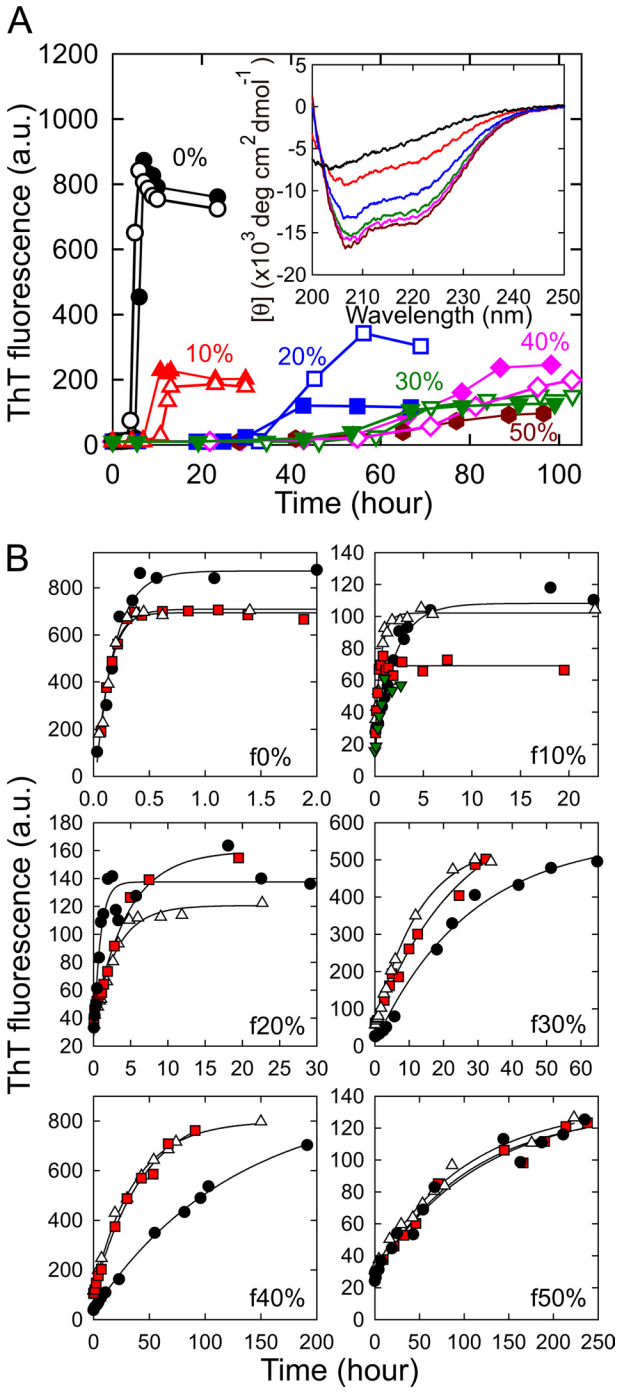

FIGURE 1. **Spontaneous formation and extension of β2-m amyloid fibrils in the presence of various concentrations of TFE.** *A*, ultrasonication-induced fibril formation in the absence (0%) or presence (10–50%) of TFE monitored by ThT fluorescence. Concentrations of TFE are 0 (●), 10 (*red* ▲ and △), 20 (*blue* ■ and □), 30 (*green* ▼ and ▽), 40 (*magenta* ◆ and ◇), and 50% (*brown hexagons*). The results of two independent experiments are shown at 0–40% TFE to demonstrate reproducibility. The fibrils formed by the reaction shown by ▲, ■, ▼, ◆, and *brown hexagons* were used as seeds for the seed-dependent extension reactions in *B*. The *inset* represents the far-UV CD spectra of β2-m monomers monitored under the same conditions with those of fibril formation. The colors are the same as those used in the main graph. The fibrils formed at 0%, 10%, 20%, 30%, 40%, and 50% TFE are referred to as f0%, f10%, f20%, f30%, f40%, and f50%, respectively. *B*, seeding effects of f0%-f50% amyloid fibrils demonstrated by the repeated self-seeding reactions. The first (*black*), second (*white*), third (*red*), and fourth (*green* in f10%) reactions are represented. *Solid lines* indicate the theoretical curves assuming a single exponential reaction.

were referred to as f0%, f10%, f20%, f30%, f40%, and f50%, respectively.

Diversity of Amyloid Fibrils Formed at Different Concentrations of TFE—As shown in Fig. 1*B*, the f0%-f50% amyloid fibrils differed in growth kinetics as well as final ThT fluorescence intensity after the completion of growth reaction, implying the manifestation of polymorphism in the presence of TFE in a concentration-dependent manner. However, the possibility of alcohol effect on the growth rate or on the amount of formed fibrils cannot be excluded only by comparing the extension reactions monitored with different solvents, and it is thus important to check seed-dependent extension reactions in the same solvent to verify the polymorphic properties among f0%-f50% fibrils.

We examined the kinetics of seed-dependent extension reactions for all the fibrils in 10 mM HCl containing 0.1 M NaCl and 5% TFE with F1 fibrils in f0%, f20%, f30%, f40%, and f50% or F2 fibrils in f10% as seeds. As a result of seeding, fibrils, except for f50%, showed typical single-exponential kinetics without a lag phase (Fig. 2*A*), demonstrating self-propagation independent of the conditions. For f50% fibrils, ThT fluorescence increased in a single-exponential manner at a slow rate but suddenly increased after 20 h of incubation (Fig. 2*A*, *inset*), presumably caused by the secondary nucleation of different fibrils as a result of the weak self-propagating ability. Consequently, f50% fibrils were precluded from investigations hereafter.

As expected, the extension rate differed notably among f0%-f40% fibrils even under the same solvent conditions (Fig. 2*A*). Although f30% and f40% showed significantly faster extension in the aqueous solution than in the presence of TFE, indicating that TFE concentration alters their growth kinetics, their rate constants under the same aqueous conditions still exhibited distinct values from that of f0%, which confirms the structural polymorphism. Interestingly, the extension rate tends to be slower in the amyloid fibrils when generated at higher TFE concentrations, as shown in Fig. 2*B*. Furthermore, the final intensity of ThT fluorescence for each type of fibril was quite similar to that observed in Fig. 1*B* (Fig. 2*A*). Although ThT fluorescence intensity usually contains a considerable amount of fluctuation, the average values of three independent experiments starting from distinct F0 fibrils were 720 ± 159 in f0%, 171 ± 50 in f10%, 275 ± 209 in f20%, 618 ± 139 in f30%, and 635 ± 123 in f40%, still representing diversity in ThT fluorescence intensity. If it is assumed that ThT fluorescence is determined by the affinity of ThT-binding sites, the number of ThT-binding sites, and ThT fluorescence strength for each bound state as well as the amount of fibrils, differences in fluorescence intensity imply conformational differences in the TFE-generated amyloid fibrils. Indeed, the measurements of critical monomer concentration (CMC) after the completion of seed-dependent extension reactions indicated that almost all of the proteins converted to fibrils (supplemental Fig. S2), supporting the structural polymorphism originating at different TFE concentrations.

Morphology and Structure of Amyloid Fibrils Generated in TFE—To explore the conformational differences among f0%-f40% amyloid fibrils in terms of morphology, the fibril products induced to extend under the same conditions (Fig. 2*A*) were

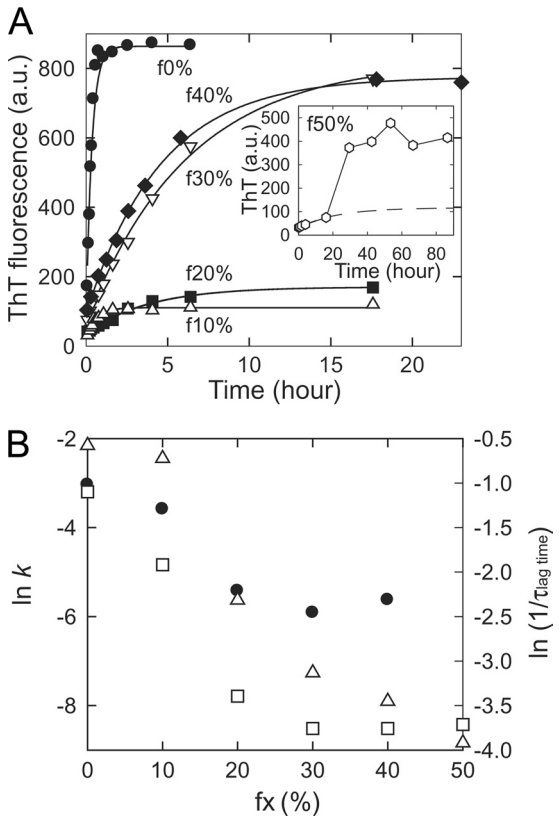

FIGURE 2. **Self-propagation of amyloid fibrils originating from various concentrations of TFE observed in an aqueous solution.** *A*, the seed-dependent extension reactions of f0%-f50% amyloid fibrils carried out in a 10 mM HCl solution containing 0.1 M NaCl and 5% TFE. In the reactions, 30 μg/ml of F1 fibrils in f0%, f20%, f30%, f40%, and f50%, or F2 fibrils in f10% were seeded. The results of f0% (●), f10% (△), f20% (■), f30% (▽), and f40% (♦) are shown, and *continuous lines* indicate the theoretical curves assuming a single exponential reaction. The *inset* shows the extension of f50% (*open hexagons*) in which the single-exponential pattern could not be observed, presumably because of the weakness of its ability for self-propagation. The *dashed line* indicates the theoretical curve of the single exponential reaction of f50% estimated by using the plots from 0 to 20 h. *B*, apparent rate constants of fibril extension of f0%-f40% at 5% TFE (●) plotted against the concentration of TFE at which fibrils originally nucleated. They were obtained by analyzing the plots in *A* with pseudo-single-exponential kinetics assuming all proteins are converted to fibrils after the saturation of ThT fluorescence intensity. The lag time of the spontaneous fibrillation (●, ■, ▼ and ♦ in 1*A*) and the rate constant of the second/third cycles of repeated self-seeding of f0% and f20–40%/f10% at original TFE concentrations (see Fig. 1*B*) are also plotted by □ and △, respectively.

subjected to transmission electron microscopy. All of the amyloid fibrils showed a needle-like morphology typical of β2-m amyloid fibrils without any amorphous aggregates. Although several apparent morphological differences have been reported in β2-m, such as rod-like and worm-like immature fibrils produced by changing the NaCl concentration or pH (33, 34), no dramatic differences in fibril length or width were observed among f0%-f40% fibrils (Fig. 3). However, patterns of the lateral assembly of protofilaments seemed somewhat different as judged by the interval of twists. Compared with f0% fibrils in which ~100 nm separated most twists, although several types were detected as reported by Kad *et al.* (35) (Fig. 3*A*), f10% fibrils showed markedly shorter intervals (Fig. 3*B*). In contrast, the repeat distance between twists seemed longer for f20%-f40% fibrils than f0% fibrils, and in f30% and f40% fibrils, an untwisted shape emerged in addition to the loosely twisted fibrils (Fig. 3, *C–E*). The distribution of repeat distances of each type of fibrils justified the difference in twists among f0%-f40% fibrils as well as the coexistence of diverse distances within one type of fibrils (Fig. 3*F*, see also supplemental Fig. S3 for details).

Although it is generally considered that the morphology of fibrils is inherited through the generations of seed-dependent fibril growth, there is a possibility that the morphologies of f30% and f40% would change with generation because marked acceleration of fibril growth during the repeated cycles of seeding, *i.e.* maturation, was observed (Fig. 1*B*) (30). However, we could not verify it, as the F0 fibrils were very short in length because of the effect of ultrasonication to break fibrils into fragments (25).

To evaluate microscopic differences in conformation, f0%-f40% fibrils produced in 10 mM HCl, 0.1 M NaCl, and 5% TFE were subjected to FTIR, CD, tryptophan fluorescence, and ANS binding measurements. For the subsequent measurements, F2 and F3 fibrils were used for f0% and f20–40%, and f10%, respectively, and the concentration of fibrils was regarded to be equal to the initial concentration of monomers present inside the sample liquid because the monomers in the sample liquid were almost depleted after the completion of fibril growth reaction (see supplemental Fig. S2).

FTIR spectra on the amide I region exhibited a sharp band with a shoulder at around 1630 cm^{-1} and 1660 cm^{-1}, respectively, for all types of the fibrils, revealing the dominance of an intermolecular β-sheet with a small amount of turn and/or loop structures (Fig. 4*A*). Intriguingly, although the spectra of f10%-f40% fibrils were overlapped almost completely, that of f0% showed some deviation from them. The difference FTIR absorption spectrum plotted by subtracting the spectrum of f10% fibrils from that of f0% fibrils showed that f10% contains larger amount of intermolecular β-sheet with a band at 1630 cm^{-1} and a smaller amount of turn and random structures with bands at 1663 cm^{-1} and 1644 cm^{-1}, respectively, than f0% (Fig. 4*B*). Considering that most residues in the middle of the molecule are incorporated in a highly organized cross-β core of amyloid fibrils in the f0% fibrils, as revealed by the previous hydrogen/deuterium exchange study (36), it is expected that the f10%-f40% fibrils generating in the presence of TFE even have a larger amount of cross-β core extending to N- and/or C-terminal regions than that of f0% fibrils.

The far-UV CD spectra also exhibited broadly a similar shape with a large minimum at ~218 nm typical of amyloid fibrils, but their intensities are various, particularly prominent under the conditions in the presence of TFE (Fig. 4*C*). The amount of fibrils inside the sample mixture is almost identical among all types of fibrils according to the fraction of β2-m monomers remaining inside the supernatant after the completion of fibril growth reaction (~10% at most, see supplemental Fig. S2), and, thus, the variability of intensity is presumably due to the propensity of fibril to aggregate forming clumps, rendering a quantitative analysis difficult. In the aqueous solution, on the other hand, the turbidity seemed to be ameliorated, but f20% showed a slight deviation with a shoulder at around 208 nm (Fig. 4*D*). Although the significance of this deviation is unknown, the intensity at 218 nm in f20% was almost the same as those of the other types of fibrils.

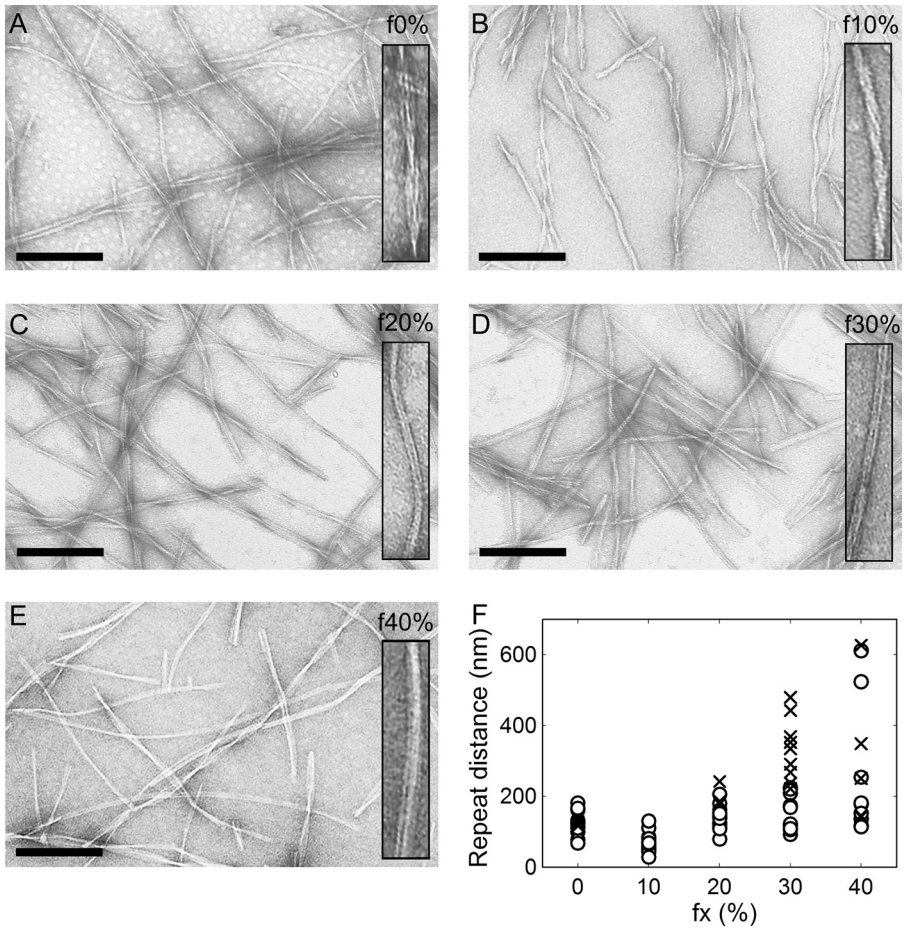

FIGURE 3. **Electron micrographs of β2-m amyloid fibrils originating from various concentrations of TFE.** f0% (*A*), f10% (*B*), f20% (*C*), f30% (*D*), and f40% (*E*). The samples of amyloid fibrils were formed by seed-dependent extension in an aqueous solution (*i.e.* 10 mM HCl containing 0.1 M NaCl and 5% TFE, see Fig. 2*A*). *Scale bars* = 200 nm. The *inset* represents an example of twisting patterns in each condition at twice the magnification in the main panel. *F*, scatter plot of the quantified repeat distances of f0%-f40% fibrils. The number of sampled amyloid fibrils was 19, 23, 18, 21, and 14 for f0%, f10%, f20%, f30%, and f40%, respectively. For each fibril, repeat distance was calculated from spaces sandwiched by crossover points (○). For fibrils with no or only one pitch in the visual field, tentative repeat distance was obtained by measuring a distance between two fibril ends or between the crossover point and fibril end (*crosses*). See supplemental Fig. S3 for more detailed procedures.

β2-m has two tryptophan residues at positions 60 and 95, the fluorescence spectrum of which has been demonstrated to be useful for studying detailed microscopic structures of amyloid fibrils (37, 38). Indeed, the tryptophan fluorescence spectra showed various patterns differing in intensity and maximum wavelength (Fig. 4*E*), revealing the conformational diversity of the f0%-f40% fibrils. The f0% amyloid fibrils showed a similar shape to the conventional fibrils formed at low pH (37), with a maximum wavelength at 348 nm (Fig. 4*E*). In contrast, f10%-f40% fibrils showed marked quenching with shorter maximum wavelengths at 332 nm, 340 nm, 340 nm, and 339 nm, respectively (Fig. 4*E*), indicating that the tryptophan residues are more buried and additionally located in the proximity of quenchers inside the proteins like the disulfide bond. The f10% fibrils showed the shortest maximum wavelength, whereas the f20%-f40% fibrils showed values intermediate between those for f0% and f10% fibrils, being roughly coupled with the pattern of morphological differences observed in the electron micrograph images (Fig. 4*E*).

The ANS fluorescence spectra of f0%-f40% also showed various intensities reflecting the diversity in surface properties of amyloid fibrils. ANS is a fluorescence probe known to bind to water-accessible hydrophobic regions. Compared with f0% fibrils, f10%-f40% fibrils showed higher intensities accompanied by slightly shorter maximum wavelengths (Fig. 4*F*), indicating that hydrophobic residues are more exposed in the fibrils generated in TFE. The slightly attenuated affinity of ANS for f20%-f40% fibrils compared with that for f10% fibrils may suggest that hydrophobic interactions are further weakened in stronger hydrophobic solvents, even disrupting the clustering of hydrophobic residues on the surface of the protein.

Stability against Gdn-HCl, Neutral pH, and Low NaCl Concentration of Amyloid Fibrils—It has been revealed that β2-m amyloid fibrils formed at low pH are depolymerized by high concentrations of Gdn-HCl (39), neutral pH (40), or low concentrations of NaCl at acidic pH (41). To address the difference in structural stability among f0%-f40% fibrils, we examined the equilibrium transition of unfolding against the concentration of Gdn-HCl and time-dependent behavior of unfolding at neutral pH or a low NaCl concentration at acidic pH. For the stability analyses, F2 and F3 fibrils formed in an aqueous solution (5% TFE) were used for f0% and f20–40%, and f10%, respectively.

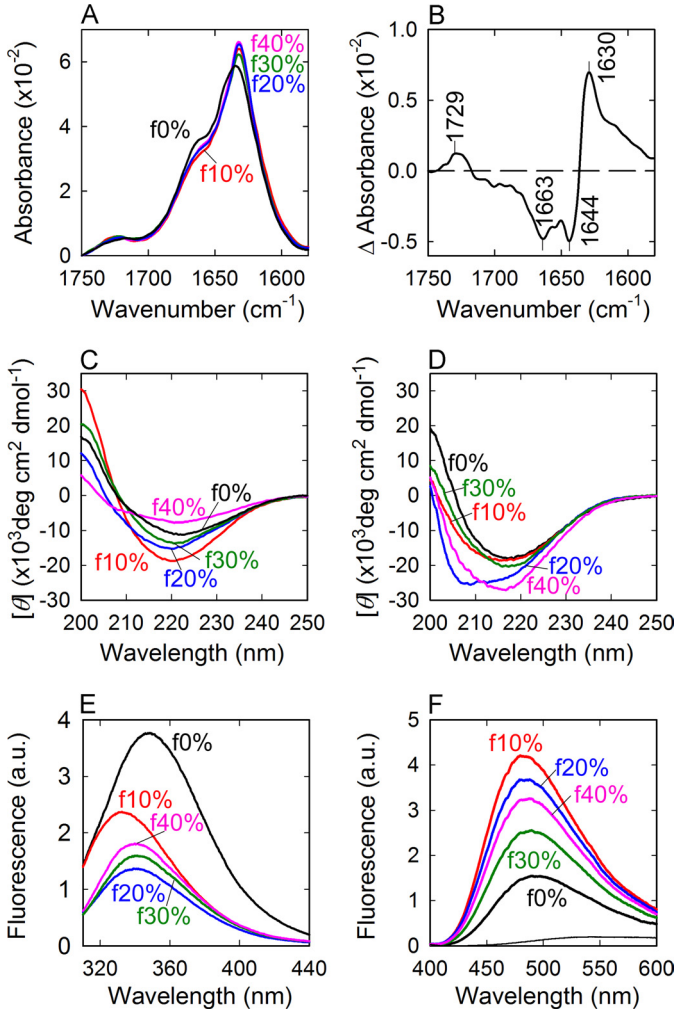

FIGURE 4. **FTIR absorption, Far-UV CD, tryptophan, and ANS fluorescence spectra of β2-m amyloid fibrils originating from various concentrations of TFE.** *A*, FTIR absorption spectra of f0% (*black*), f10% (*red*), f20% (*blue*), f30% (*green*), and f40% (*magenta*) amyloid fibrils formed by the seed-dependent extension reactions in an aqueous solution (5% TFE). *B*, difference FTIR spectrum subtracting the spectrum of f0% from that of f10%. *C* and *D*, CD spectra of amyloid fibrils formed by the seed-dependent extension in TFE (*C*) and in an aqueous solution (*D*). The spectra of f0% (*black*), f10% (*red*), f20% (*blue*), f30% (*green*), and f40% (*magenta*) are shown in each panel. *E* and *F*, tryptophan fluorescence (*E*) and ANS fluorescence spectra (*F*) of f0% (*black*), f10% (*red*), f20% (*blue*), f30% (*green*), and f40% (*magenta*) amyloid fibrils formed by seed-dependent extension in the aqueous solution. The thin line in *F* represents a reference ANS spectrum in the absence of fibrils. All of the measurements were performed at 25 °C.

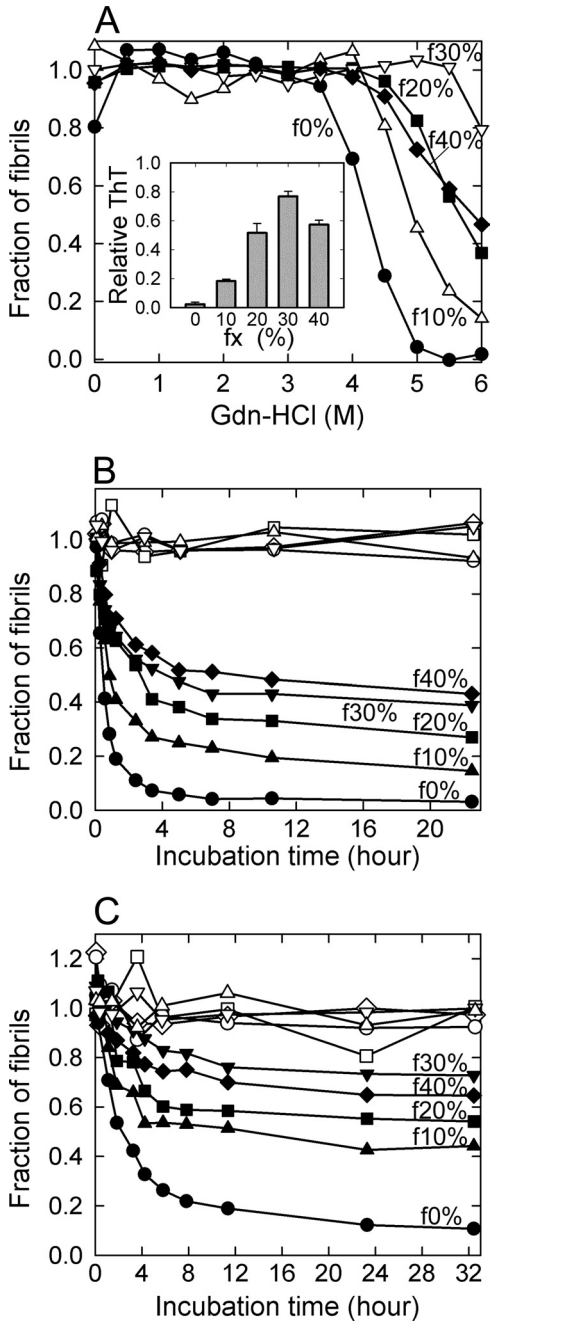

FIGURE 5. **Stability of β2-m amyloid fibrils originating from various concentrations of TFE.** *A*, thermodynamic stability against Gdn-HCl. The fibrils were incubated overnight in the presence of various concentrations of Gdn-HCl at 25 °C, and the fraction of residual fibrils was obtained by the change in the intrinsic tryptophan fluorescence spectrum (see "Experimental Procedures" and supplemental Fig. S4). Fibrils are f0% (●), f10% (△), f20% (■), f30% (▽), and f40% (♦), all of which were formed by the seed-dependent extension in the aqueous solution. The *inset* shows the relative ThT fluorescence intensity at 6 M Gdn-HCl, assuming the value at 0 M Gdn-HCl to be 1, which coincided well with the fraction of fibrils estimated from tryptophan fluorescence. *B* and *C*, stability against neutral pH (*B*) and desalted conditions (*C*). The depolymerization reaction was initiated by varying the pH to 7 (*B*) or NaCl concentration to 4.2 mM (*C*). Fibrils are f0% (●), f10% (▲), f20% (■), f30% (▼), and f40% (♦), all of which were formed by the seed-dependent extension in the aqueous solution. The reactions were monitored by the ThT fluorescence, and the ordinate is converted to the fraction of remaining fibrils in this figure. ○, △, □, ▽, and ◇ represent the time courses of fibrils without any jump in pH (*B*) or NaCl concentration (*C*) for a control.

When the Gdn-HCl-induced unfolding was analyzed by the change of $<\nu>$ values calculated from the tryptophan fluorescence spectra against the concentration of Gdn-HCl, all of the fibrils revealed cooperative unfolding transitions (Fig. 5*A* and supplemental Fig. S4). Intriguingly, the apparent C_m values of f10%-f40% fibrils shifted markedly to higher Gdn-HCl concentrations compared with those of f0% fibrils. The stability increased in the order f0% < f10% < f20% ≈ f40% < f30%, with ~80% of the initial amount of f30% fibrils surviving even at 6 M Gdn-HCl (Fig. 5*A*). Although the f40% fibrils showed a slight deviation, the results indicate that amyloid fibrils gain structural stability as they nucleate at higher concentrations of TFE.

When f0% fibrils were incubated at pH7.0 or at a low concentration of NaCl (4.2 mM) in 10 mM HCl (pH ~2), ThT fluores-

cence decreased immediately toward the control value obtained without fibrils, showing almost complete depolymerization in accordance with previous reports (40, 41) (Fig. 5, *B* and *C*). In the case of f10%-f40% amyloid fibrils, on the other hand, the ThT fluorescence indicated that significant amounts of the fibrils remained after the depolymerization reactions (Fig. 5, *B* and *C*). If it is assumed that depolymerization reaction proceeds according to a simple thermodynamic scheme with the dynamic nature between the monomeric dissociation and association occurring at the end of each fibril, the final intensity in ThT fluorescence is attributed to a fraction of original fibrils surviving at equilibrium. The amount that remained increased in the order f0% < f10% <f20% <f30% ≈ f40% at both neutral pH and a low NaCl concentration, and ~40% of both f30% and f40% remained at neutral pH and 70% at a low NaCl concentration. The order of stability was similar to that observed in Gdn-HCl-induced unfolding, indicating that the amyloid fibrils nucleating at higher TFE concentrations gain higher tolerance against the perturbation of ionic strength as well as global conformational stability.

To obtain insights into packing density inside f0%-f40% amyloid fibrils, we further examined pressure responses of these fibrils by monitoring tryptophan fluorescence spectra at different levels of pressure during the compression process. Pressure is a thermodynamic perturbant that shifts equilibration toward a smaller systematic volume, thereby providing insights into packing density inside amyloid fibrils. We have previously revealed the loosely packed structure of β2-m fibrils by observing a pressure-induced structural reorganization toward a more packed structure (42), on the basis of which it is considered that pressure response is useful as an indicator of loosely packed amyloid structure containing water-inaccessible voids. In this case, pressurization caused no response in f20%-f40%, whereas a cooperative pressure-induced conformational transition occurred in f0% and f10% fibrils, indicating the elimination of packing defects in fibrils formed at higher concentrations of TFE (see supplemental Fig. S5 and Methods for details).

DISCUSSION

Formation of Amyloid Fibrils in TFE—We obtained various types of amyloid fibrils of β2-m at different concentrations of TFE up to 50%. The main effect of TFE is expected to be a weakening of hydrophobic interactions with a strengthening of electrostatic interactions (including polar and charge-charge interactions) that leads to denaturation of the rigid native structure of proteins (43, 44) and stabilization of the α-helical structure (45, 46). Especially at higher concentrations of TFE, the α-helical structure is dominant with intramolecularly stabilized hydrogen bond networks, whereas little intermolecular association or aggregation. By utilizing this effect, TFE has been used to dissolve amyloid fibrils, including β2-m (32). However, we have demonstrated that, in TFE, amyloid fibrils can be formed even at high alcohol concentrations if the protein solution is irradiated with ultrasonic waves to accelerate the fibril-forming process (Fig. 1).

In our previous studies, ultrasonication was proven to enhance the spontaneous formation of amyloid fibrils (25–27). Ultrasonic waves produce microbubbles that repeatedly grow and collapse in synchrony with the driving ultrasonic amplitude. The large shearing forces generated by the cavitation-induced solvent flow are predominantly responsible for the fragmentation of preformed long fibrils. On the other hand, the exact mechanism for the induction of fibrillation is still unclear, but it seems that the aggregated denatured proteins accumulated at the air-liquid interface of microbubbles provide templates (*i.e.* nuclei) for fibril growth (27). In this case, these strong effects of agitation by ultrasonication allowed β2-m to exceed a very high energy barrier to nucleate from the α-helical structure in TFE, resulting in the emergence of novel types of amyloid fibrils. It is thus suggested that ultrasonication is a useful tool to reveal amyloid fibrils potentially hidden by the high energetic barrier of the nucleation process.

Relationship between Fibril Polymorphism and Hydrophobic Interactions—As for the polymorphic features of β2-m fibrils reported so far, several distinct forms are known to be produced, depending on experimental conditions such as the concentration of salt (15, 33, 34, 47), pH (30, 33), and the reduction of disulfide bonds (48). Although the polymorphic structure caused by the pH and NaCl concentration suggests a role for electrostatic interactions in determining fibril structure, it has not been clarified what characteristics of side chain interactions influence the resulting fibril structure most critically. In this study, the f0% to f40% fibrils exhibited various kinetic and thermodynamic properties dependent on the concentration of TFE. Notably, there was a rough negative correlation between the extension rate and concentration of TFE at which fibrils are initially generated, which implies a major contribution of hydrophobic interactions to the acceleration of fibrillation kinetics (Fig. 2). Furthermore, thermodynamic stability also showed a significant correlation. Intriguingly, the direction of the correlation was opposite to that for the kinetic property, and more stable fibrils were formed at higher concentrations of TFE, as judged by the thermodynamic study of Gdn-HCl and desalting of NaCl, although f40% showed slight deviation (Fig. 5). Overall, the sensitivity of the structural polymorphism to the concentration of TFE implies that the balance of hydrophobic and electrostatic interactions is essential to the manifestation of polymorphic f0%-f40% amyloid fibrils.

From the results of FTIR spectroscopy, we considered that all of the TFE-derived amyloid fibrils have a large amount of cross-β structure over most of the protein sequence (36). Unlike the flexible filamentous form of β2-m amyloid fibrils called "immature fibrils" or "worm-like fibrils" with smaller regions of the cross-β core, the structural differences among f0%-f40% seems attributable to residue-level conformational differences inside the cross-β core in addition to minute difference in extent of the cross-β structures contained in the fibrils between f0% and f10%-f40% fibrils. This interpretation seems consistent with the rigid needle-like morphology with a similar fibril width but different ThT intensity and tryptophan fluorescence spectrum. Moreover, the fluorescence intensity of ANS, a probe for hydrophobic regions on the surface of a protein, suggested the hydrophobic residues to be more exposed in the fibrils generated at higher TFE concentrations. Side chains, especially hydrophobic residues, are likely to play an essential role in affecting first the structure and then properties like sta-

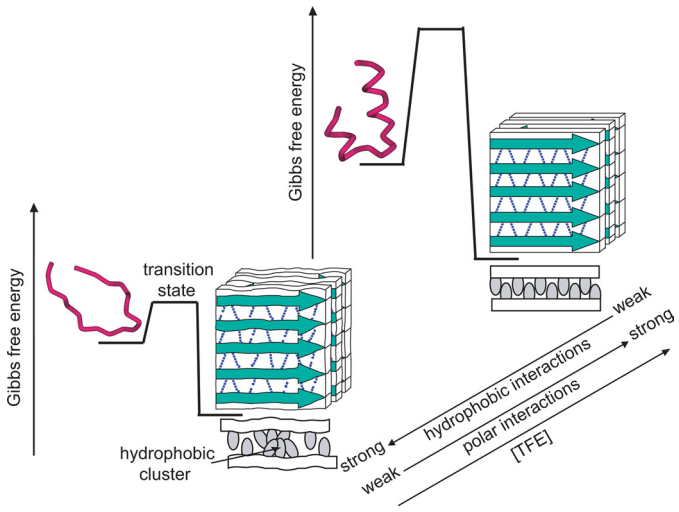

FIGURE 6. **Schematic representation for the mechanism by which polymorphic forms of β2-m amyloid fibrils develop at various concentrations of TFE.** With the structural illustrations for the monomeric and amyloid forms, free energy profiles for the formation of β2-m amyloid fibrils at low (*left*) and high (*right*) concentrations of TFE are shown. For the illustrations of amyloid fibrils, peptide backbones and hydrogen bond networks are represented by *green arrows* and *dotted lines*, respectively, and the stacking pattern of β-strands is tentatively represented as a parallel structure. The top-view model is also shown at the bottom of each fibril model to represent patterns of side chains (*gray ovals*) between the two cross-β sheets (*white bars*).

bility and kinetics. This idea aligns with the recent proposal that the formation of several patterns of side chain docking is one of the structural bases underlying the amyloid polymorphism in studies using x-ray crystallography and microcrystals (16, 18).

Proposed Model for the Manifestation of Polymorphism in TFE—On the basis of this observation, a schematic model explaining the polymorphism at various concentrations of TFE is summarized in Fig. 6. The structure of amyloid fibrils has been expected to be determined predominantly by the hydrogen bond network in the extended intermolecular β-sheet structure of the peptide backbones, the side chain interactions bearing a secondary role (42, 49). With this unique architecture of amyloid fibrils, too many side chain interactions, especially hydrophobic interactions, have an adverse effect on the main chain hydrogen bond network and occasionally cause the distortion of cross-β sheets with a lot of void spaces (Fig. 6, *left*). Although detailed positions or sizes of voids have not been specified, the presence of void spaces in the conventional β2-m fibrils formed in aqueous solutions has been revealed previously by the structural sensitivity to pressurization (42) as well as the thermodynamic parameters obtained through isothermal titration calorimetry (50) and by the partial molar volume obtained through densitometry (51). In such circumstances, TFE is expected to diminish the contribution of side chain hydrophobic interactions relative to that of the main chain hydrogen bonds by decreasing and increasing hydrophobic and polar interactions of polypeptide chains, respectively, in a concentration-dependent manner, resulting in a decrease in structural deficiencies which is accompanied by a slight increase in content of cross-β core regions. At a high concentration of alcohol, unfavorable hydrophobic interactions are almost negligible, achieving a non-defective cross-β structure without main chain distortions (Fig. 6, *right*).

The above model is consistent with the insensitivity to pressurization in f20%-f40% fibrils (supplemental Fig. S5). The untwisted shape observed at higher concentrations of TFE (Fig. 3) may also support the formation of a more idealized cross-β structure containing minimum distortion. We expected that some variation in hydrogen bonding strength was indicated by different frequency of the intermolecular β-sheet band in the FTIR spectrum, but no significant difference was found within the limit of spectral resolution. This result suggests that even imperceptible or partial variation in cross-β architecture exerts strong influence on the nature of amyloid fibrils. The slightly different characteristics of f10%, *i.e.* a remarkably twisted morphology and the burial of tryptophan residues that are uncoupled with a linear decrease in hydrophobic interactions predicted with an increase in the concentration of TFE would be caused by the complicated mechanism of TFE action, forming dynamic clusters that directly binds protein molecules observed specifically below the alcohol clustering concentration (23, 24, 45).

When the heterogeneity in morphology found in all types of fibrils is considered, each polymorph might be manifested by a competitive amplification of one subpopulation of fibrils already present to some extent in the conventional f0% fibrils. However, we could not verify this possibility because too diverse a morphology in terms of repeat distance was observed and it was quite difficult to separate morphology types (Fig. 3).

Implications for the Manifestation of Polymorphism in Vivo—In conclusion, our results have newly revealed the ability of β2-m to form amyloid fibrils with a stable cross-β structure even in a hydrophobic solvent like TFE. Although destruction of the native structure and generation of the α-helix have been emphasized as a role of TFE, our results shed light on another aspect: that a stable cross-β structure can be formed concomitantly only if a high-energy barrier is cleared, leading to the novel concept that the α-helix and cross-β sheet are two sides of the same coin. This idea is acceptable if one notes that both structures are stabilized by extended networks of hydrogen bonds. The change from the α-helix to cross-β structure is thus considered a simple process in which intramolecular hydrogen bonds are recombined to produce intermolecular bonds.

The close relationship between the α-helix and cross-β structure further provides support for the recent experimental findings that the biomembrane-bound α-helical structure plays a role as a fibrillating intermediate in several disordered proteins or peptides such as islet amyloid polypeptide and amyloid-β peptides (52, 53). Although the formation of α-helical structures prior to the organization of cross-β appears paradoxical at first glance, these α-helical structures plausibly have the potential to form amyloid structures that has been acquired by association with the biological membrane. Alcohol bears a resemblance to lipid molecules constituting the membrane surface. Although details of polymorphism of β2-m amyloid fibrils manifested *in vivo* have not been revealed, with only one example originally derived from the joints of a patient whose characteristics seems roughly analogous to those of f0% fibrils (see supplemental Fig. S5), it is likely that different external perturbations, such as membrane lipid composition or other coexisting materials, are expected to serve as the driving force in the

manifestation of polymorphism. Identifying such biological factors will be important to obtain further insight into the molecular mechanism *in vivo*. On the basis of the above observations, an idealized α-helix is considered an important indicator of an insurmountable energetic barrier of fibrillation, and administration of chemical compounds rendering polypeptide chains toward a more idealized α-helix will thus become another novel therapeutic strategy for alleviating the propagation of amyloid fibrils at a molecular level.

Acknowledgments—We thank Y. Kobayashi for the expression and purification of recombinant β2-m protein. We also thank Drs. N. Yamamoto and K. Tominaga (Kobe University) for support of FTIR measurements. Electron micrographs were recorded using a facility in the Research Center for Ultrahigh Voltage Electron Microscopy, Osaka University.

REFERENCES

1. Rochet, J. C., and Lansbury, P. T., Jr. (2000) Amyloid fibrillogenesis. Themes and variations. *Curr. Opin. Struct. Biol.* **10,** 60–68
2. Cohen, F. E., and Kelly, J. W. (2003) Therapeutic approaches to protein misfolding diseases. *Nature* **426,** 905–909
3. Dobson, C. M. (2003) Protein folding and misfolding. *Nature* **426,** 884–890
4. Uversky, V. N., and Fink, A. L. (2004) Conformational constraints for amyloid fibrillation. The importance of being unfolded. *Biochim. Biophys. Acta* **1698,** 131–153
5. Tanaka, M., Chien, P., Naber, N., Cooke, R., and Weissman, J. S. (2004) Conformational variations in an infectious protein determine prion strain differences. *Nature* **428,** 323–328
6. Paravastu, A. K., Leapman, R. D., Yau, W. M., and Tycko, R. (2008) Molecular structural basis for polymorphism in Alzheimer's β-amyloid fibrils. *Proc. Natl. Acad. Sci. U.S.A.* **105,** 18349–18354
7. Nekooki-Machida, Y., Kurosawa, M., Nukina, N., Ito, K., Oda, T., and Tanaka, M. (2009) Distinct conformations of *in vitro* and *in vivo* amyloids of huntingtin-exon1 show different cytotoxicity. *Proc. Natl. Acad. Sci. U.S.A.* **106,** 9679–9684
8. Kodali, R., and Wetzel, R. (2007) Polymorphism in the intermediates and products of amyloid assembly. *Curr. Opin. Struct. Biol.* **17,** 48–57
9. Anderson, M., Bocharova, O. V., Makarava, N., Breydo, L., Salnikov, V. V., and Baskakov, I. V. (2006) Polymorphism and ultrastructural organization of prion protein amyloid fibrils. An insight from high-resolution atomic force microscopy. *J. Mol. Biol.* **358,** 580–596
10. Yamaguchi, K., Katou, H., Hoshino, M., Hasegawa, K., Naiki, H., and Goto, Y. (2004) Core and heterogeneity of β_2-microglobulin amyloid fibrils as revealed by H/D exchange. *J. Mol. Biol.* **338,** 559–571
11. Toyama, B. H., Kelly, M. J., Gross, J. D., and Weissman, J. S. (2007) The structural basis of yeast prion strain variants. *Nature* **449,** 233–237
12. Madine, J., Jack, E., Stockley, P. G., Radford, S. E., Serpell, L. C., and Middleton, D. A. (2008) Structural insights into the polymorphism of amyloid-like fibrils formed by region 20–29 of amylin revealed by solid-state NMR and X-ray fiber diffraction. *J. Am. Chem. Soc.* **130,** 14990–15001
13. Petkova, A. T., Leapman, R. D., Guo, Z., Yau, W. M., Mattson, M. P., and Tycko, R. (2005) Self-propagating, molecular-level polymorphism in Alzheimer's β-amyloid fibrils. *Science* **307,** 262–265
14. Heise, H., Hoyer, W., Becker, S., Andronesi, O. C., Riedel, D., and Baldus, M. (2005) Molecular-level secondary structure, polymorphism, and dynamics of full-length α-synuclein fibrils studied by solid-state NMR. *Proc. Natl. Acad. Sci. U.S.A.* **102,** 15871–15876
15. Debelouchina, G. T., Platt, G. W., Bayro, M. J., Radford, S. E., and Griffin, R. G. (2010) Magic angle spinning NMR analysis of β_2-microglobulin amyloid fibrils in two distinct morphologies. *J. Am. Chem. Soc.* **132,** 10414–10423
16. Meinhardt, J., Sachse, C., Hortschansky, P., Grigorieff, N., and Fändrich, M. (2009) Aβ(1–40) fibril polymorphism implies diverse interaction patterns in amyloid fibrils. *J. Mol. Biol.* **386,** 869–877
17. Sawaya, M. R., Sambashivan, S., Nelson, R., Ivanova, M. I., Sievers, S. A., Apostol, M. I., Thompson, M. J., Balbirnie, M., Wiltzius, J. J., McFarlane, H. T., Madsen, A. Ø., Riekel, C., and Eisenberg, D. (2007) Atomic structures of amyloid cross-β spines reveal varied steric zippers. *Nature* **447,** 453–457
18. Wiltzius, J. J., Landau, M., Nelson, R., Sawaya, M. R., Apostol, M. I., Goldschmidt, L., Soriaga, A. B., Cascio, D., Rajashankar, K., and Eisenberg, D. (2009) Molecular mechanisms for protein-encoded inheritance. *Nat. Struct. Mol. Biol.* **16,** 973–978
19. Jones, E. M., and Surewicz, W. K. (2005) Fibril conformation as the basis of species- and strain-dependent seeding specificity of mammalian prion amyloids. *Cell* **121,** 63–72
20. Andersen, C. B., Hicks, M. R., Vetri, V., Vandahl, B., Rahbek-Nielsen, H., Thøgersen, H., Thøgersen, I. B., Enghild, J. J., Serpell, L. C., Rischel, C., and Otzen, D. E. (2010) Glucagon fibril polymorphism reflects differences in protofilament backbone structure. *J. Mol. Biol.* **397,** 932–946
21. Yamamoto, S., and Gejyo, F. (2005) Historical background and clinical treatment of dialysis-related amyloidosis. *Biochim. Biophys. Acta* **1753,** 4–10
22. Giorgetti, S., Raimondi, S., Pagano, K., Relini, A., Bucciantini, M., Corazza, A., Fogolari, F., Codutti, L., Salmona, M., Mangione, P., Colombo, L., De Luigi, A., Porcari, R., Gliozzi, A., Stefani, M., Esposito, G., Bellotti, V., and Stoppini, M. (2011) Effect of tetracyclines on the dynamics of formation and destructuration of β_2-microglobulin amyloid fibrils. *J. Biol. Chem.* **286,** 2121–2131
23. Yamaguchi, K., Naiki, H., and Goto, Y. (2006) Mechanism by which the amyloid-like fibrils of a β_2-microglobulin fragment are induced by fluorine-substituted alcohols. *J. Mol. Biol.* **363,** 279–288
24. Yanagi, K., Ashizaki, M., Yagi, H., Sakurai, K., Lee, Y. H., and Goto, Y. (2011) Hexafluoroisopropanol induces amyloid fibrils of islet amyloid polypeptide by enhancing both hydrophobic and electrostatic interactions. *J. Biol. Chem.* **286,** 23959–23966
25. Ohhashi, Y., Kihara, M., Naiki, H., and Goto, Y. (2005) Ultrasonication-induced amyloid fibril formation of β_2-microglobulin. *J. Biol. Chem.* **280,** 32843–32848
26. Chatani, E., Lee, Y. H., Yagi, H., Yoshimura, Y., Naiki, H., and Goto, Y. (2009) Ultrasonication-dependent production and breakdown lead to minimum-sized amyloid fibrils. *Proc. Natl. Acad. Sci. U.S.A.* **106,** 11119–11124
27. So, M., Yagi, H., Sakurai, K., Ogi, H., Naiki, H., and Goto, Y. (2011) Ultrasonication-dependent acceleration of amyloid fibril formation. *J. Mol. Biol.* **412,** 568–577
28. Chiba, T., Hagihara, Y., Higurashi, T., Hasegawa, K., Naiki, H., and Goto, Y. (2003) Amyloid fibril formation in the context of full-length protein. Effects of proline mutations on the amyloid fibril formation of β_2-microglobulin. *J. Biol. Chem.* **278,** 47016–47024
29. Naiki, H., Hashimoto, N., Suzuki, S., Kimura, H., Nakakuki, K., and Gejyo, F. (1997) Establishment of a kinetic model of dialysis-related amyloid fibril extension *in vitro*. *Amyloid* **4,** 223–232
30. Kihara, M., Chatani, E., Sakai, M., Hasegawa, K., Naiki, H., and Goto, Y. (2005) Seeding-dependent maturation of β_2-microglobulin amyloid fibrils at neutral pH. *J. Biol. Chem.* **280,** 12012–12018
31. Silva, J. L., Miles, E. W., and Weber, G. (1986) Pressure dissociation and conformational drift of the β dimer of tryptophan synthase. *Biochemistry* **25,** 5780–5786
32. Hirota-Nakaoka, N., Hasegawa, K., Naiki, H., and Goto, Y. (2003) Dissolution of β_2-microglobulin amyloid fibrils by dimethylsulfoxide. *J. Biochem.* **134,** 159–164
33. Gosal, W. S., Morten, I. J., Hewitt, E. W., Smith, D. A., Thomson, N. H., and Radford, S. E. (2005) Competing pathways determine fibril morphology in the self-assembly of β_2-microglobulin into amyloid. *J. Mol. Biol.* **351,** 850–864
34. Hong, D. P., Gozu, M., Hasegawa, K., Naiki, H., and Goto, Y. (2002) Conformation of β_2-microglobulin amyloid fibrils analyzed by reduction of the disulfide bond. *J. Biol. Chem.* **277,** 21554–21560

35. Kad, N. M., Myers, S. L., Smith, D. P., Smith, D. A., Radford, S. E., and Thomson, N. H. (2003) Hierarchical assembly of β_2-microglobulin amyloid *in vitro* revealed by atomic force microscopy. *J. Mol. Biol.* **330,** 785–797
36. Hoshino, M., Katou, H., Hagihara, Y., Hasegawa, K., Naiki, H., and Goto, Y. (2002) Mapping the core of the β_2-microglobulin amyloid fibril by H/D exchange. *Nat. Struct. Biol.* **9,** 332–336
37. Kihara, M., Chatani, E., Iwata, K., Yamamoto, K., Matsuura, T., Nakagawa, A., Naiki, H., and Goto, Y. (2006) Conformation of amyloid fibrils of β_2-microglobulin probed by tryptophan mutagenesis. *J. Biol. Chem.* **281,** 31061–31069
38. Chatani, E., Ohnishi, R., Konuma, T., Sakurai, K., Naiki, H., and Goto, Y. (2010) Pre-steady-state kinetic analysis of the elongation of amyloid fibrils of β_2-microglobulin with tryptophan mutagenesis. *J. Mol. Biol.* **400,** 1057–1066
39. Narimoto, T., Sakurai, K., Okamoto, A., Chatani, E., Hoshino, M., Hasegawa, K., Naiki, H., and Goto, Y. (2004) Conformational stability of amyloid fibrils of β_2-microglobulin probed by guanidine-hydrochloride-induced unfolding. *FEBS Lett.* **576,** 313–319
40. Yamaguchi, I., Hasegawa, K., Takahashi, N., Gejyo, F., and Naiki, H. (2001) Apolipoprotein E inhibits the depolymerization of β_2-microglobulin-related amyloid fibrils at a neutral pH. *Biochemistry* **40,** 8499–8507
41. Raman, B., Chatani, E., Kihara, M., Ban, T., Sakai, M., Hasegawa, K., Naiki, H., Rao, C. M., and Goto, Y. (2005) Critical balance of electrostatic and hydrophobic interactions is required for β_2-microglobulin amyloid fibril growth and stability. *Biochemistry* **44,** 1288–1299
42. Chatani, E., Kato, M., Kawai, T., Naiki, H., and Goto, Y. (2005) Main-chain dominated amyloid structures demonstrated by the effect of high pressure. *J. Mol. Biol.* **352,** 941–951
43. Yamamoto, S., Yamaguchi, I., Hasegawa, K., Tsutsumi, S., Goto, Y., Gejyo, F., and Naiki, H. (2004) Glycosaminoglycans enhance the trifluoroethanol-induced extension of β_2-microglobulin-related amyloid fibrils at a neutral pH. *J. Am. Soc. Nephrol.* **15,** 126–133
44. Rennella, E., Corazza, A., Giorgetti, S., Fogolari, F., Viglino, P., Porcari, R., Verga, L., Stoppini, M., Bellotti, V., and Esposito, G. (2010) Folding and fibrillogenesis. Clues from β_2-microglobulin. *J. Mol. Biol.* **401,** 286–297
45. Hirota, N., Mizuno, K., and Goto, Y. (1998) Group additive contributions to the alcohol-induced α-helix formation of melittin. Implication for the mechanism of the alcohol effects on proteins. *J. Mol. Biol.* **275,** 365–378
46. Hong, D. P., Hoshino, M. Kuboi, R., and Goto, Y. (1999) Clustering of fluorine-substituted alcohols as a factor responsible for their marked effects on proteins and peptides. *J. Am. Chem. Soc.* **121,** 8427–8433
47. McParland, V. J., Kad, N. M., Kalverda, A. P., Brown, A., Kirwin-Jones, P., Hunter, M. G., Sunde, M., and Radford, S. E. (2000) Partially unfolded states of β_2-microglobulin and amyloid formation *in vitro*. *Biochemistry* **39,** 8735–8746
48. Ohhashi, Y., Hagihara, Y., Kozhukh, G., Hoshino, M., Hasegawa, K., Yamaguchi, I., Naiki, H., and Goto, Y. (2002) The intrachain disulfide bond of β_2-microglobulin is not essential for the immunoglobulin fold at neutral pH, but is essential for amyloid fibril formation at acidic pH. *J. Biochem.* **131,** 45–52
49. Fändrich, M., and Dobson, C. M. (2002) The behaviour of polyamino acids reveals an inverse side chain effect in amyloid structure formation. *EMBO J.* **21,** 5682–5690
50. Kardos, J., Yamamoto, K., Hasegawa, K., Naiki, H., and Goto, Y. (2004) Direct measurement of the thermodynamic parameters of amyloid formation by isothermal titration calorimetry. *J. Biol. Chem.* **279,** 55308–55314
51. Lee, Y. H., Chatani, E., Sasahara, K., Naiki, H., and Goto, Y. (2009) A comprehensive model for packing and hydration for amyloid fibrils of β_2-microglobulin. *J. Biol. Chem.* **284,** 2169–2175
52. Hebda, J. A., and Miranker, A. D. (2009) The interplay of catalysis and toxicity by amyloid intermediates on lipid bilayers. Insights from type II diabetes. *Annu. Rev. Biophys.* **38,** 125–152
53. Kirkitadze, M. D., Condron, M. M., and Teplow, D. B. (2001) Identification and characterization of key kinetic intermediates in amyloid β-protein fibrillogenesis. *J. Mol. Biol.* **312,** 1103–1119